Blind Calibration of Multi-Channel Samplers using Sparse Recovery

Yuanxin Li, Yingsheng He, Yuejie Chi
Department of Electrical and Computer Engineering
The Ohio State University, Columbus, OH 43210, USA
Email: {li.3822, he.759, chi.97}@osu.edu

Yue M. Lu
School of Engineering and Applied Sciences
Harvard University, Cambridge, MA 02138, USA
Email: yuelu@seas.harvard.edu

***Abstract*—We propose an algorithm for blind calibration of multi-channel samplers in the presence of unknown gains and offsets, which is useful in many applications such as multi-channel analog-to-digital converters, image super-resolution, and sensor networks. Using a subspace-based rank condition developed by Vandewalle et al., we obtain a set of linear equations with respect to complex harmonics whose frequencies are determined by the offsets, and the coefficients of each harmonic are determined by the discrete-time Fourier transforms of outputs of each of the channels. By discretizing the offsets over a fine grid, this becomes a sparse recovery problem where the signal of interest is sparse with an additional structure, that in each block there is only one nonzero entry. We propose a modified CoSaMP algorithm that takes this structure into account to estimate the offsets. Our algorithm is scalable to large numbers of channels and can also be extended to multi-dimensional signals. Numerical experiments demonstrate the effectiveness of the proposed algorithm.**

***Index Terms*—multi-channel sampling, blind calibration, sparse recovery, CoSaMP**

I. Introduction

The time-interleaved multi-channel sampler, demonstrated in Fig. 1, is an attractive architecture for sampling wideband signals at sub-Nyquist rates without additional assumptions such as sparse spectral occupancy. It is also an important model for image super-resolution, where a high-resolution image can be reconstructed from a set of lower-resolution images that are slightly misaligned from each other. The multi-channel sampler is composed of K channels, where an input of continuous-time band-limited signal $x(t)$ is sampled in parallel using the same sampling period T, with a different offset $\tau_k \in [0, T)$ and gain $\alpha_k \in \mathbb{C}$ in each channel. When the offsets and gains of all channels are known perfectly, this coincides with the well-known Papoulis generalized sampling scheme [1], and it is possible to recover $x(t)$ by sampling each channel at $1/K$ the Nyquist rate of the input signal.

However, in practice, the gains $\{\alpha_k\}_{k=1}^K$ and offsets $\{\tau_k\}_{k=1}^K$ are typically *unknown* and must be calibrated before use. Without loss of generality, we assume $\alpha_1 = 1$ and $\tau_1 = 0$ for identifiability considerations. While it is possible to calibrate using a known input $x(t)$, it is much more desirable to calibrate the multi-channel sampler in a blind fashion without knowledge of the input signal. Many existing blind calibration approaches only included calibration of unknown offsets [2], [3] and were limited to very small number of channels (*e.g.* $K = 2, 4, 8$). These drawbacks have severely limited the adoption of the multi-channel sampler especially when the number of channels is large. More recently, Vandewalle, Lu and Vetterli [4], [5] have developed blind calibration methods including both unknown gains and offsets, based upon a subspace-based rank condition which shows that with a modest amount of oversampling, the output of the first channel in the frequency domain can be written as a *linear superposition* of the outputs of the other $(K-1)$ channels. However, their algorithms are either computationally complex by performing a matrix rank test using exhaustive search [4], or noise-sensitive due to algebraic root-finding [5]. It is also not clear how to extend the method in [5] to the two-dimensional (2D) case which becomes relevant in image super-resolution.

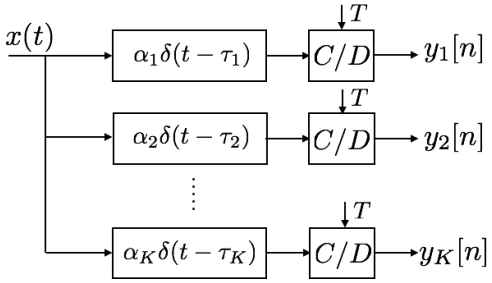

Fig. 1: The architecture of a multi-channel sampler.

In this paper, we develop an efficient algorithm for blind calibration of multi-channel samplers in the presence of both unknown gains and offsets, in the same setting studied in [4], [5]. Since the gains can be obtained by using a least-squares step once the offsets are estimated, we focus on offset estimation. We first recognize that the subspace-based rank condition can be formulated into a set of linear equations with respect to $(K-1)$ complex harmonics whose frequencies are determined by the offsets, and the coefficients of each harmonic are determined by the discrete-time Fourier transforms (DTFT) of outputs of each of the channels. By discretizing the offsets over a fine grid, this becomes a sparse recovery problem where the signal of interest is sparse with an additional structure: in each block there is only one nonzero entry. We modify the CoSaMP algorithm [6], a popular algorithm in the sparse recovery literature, to directly take this structure into account in estimating the unknown offsets. Our algorithm is scalable to multiple channels and can be extended to multi-

dimensional signals. Numerical experiments are provided to demonstrate the effectiveness of the proposed algorithm.

The rest of this paper is organized as follows. We provide background on the problem formulation in Section II, and describe the proposed algorithm in Section III. In Section IV, we provide numerical experiments to validate the performance of the proposed algorithm. We conclude in Section V. Throughout the paper, $(\cdot)^T$ denotes matrix transpose, $(\cdot)^H$ denotes the conjugate transpose, $(\cdot)^\dagger$ denotes the pseudo-inverse, and $\odot$ denotes the Hadamard product.

II. Background on Multi-Channel Samplers

Denote the continuous-time Fourier transform (CTFT) of $x(t)$ as $X(\omega) = \int x(t)e^{-j\omega t}dt$. We consider band-limited $x(t)$, in which case $X(\omega)$ is supported within the band $[-B, B]$, for some $B > 0$. As in Fig. 1, in each channel we sample $x(t)$ uniformly at a rate $\frac{1}{T} < \frac{B}{\pi}$. The subsampling ratio per channel is $S = \frac{BT}{\pi}$. Then the samples from the kth channel can be represented as

$$y_k[n] = \alpha_k x(nT - \tau_k), \tag{1}$$

for $k = 1, 2, \ldots, K$. The DTFT of $y_k[n]$'s is given as

$$\begin{aligned} Y_k(\omega) &= \sum_{n\in\mathbb{Z}} y_k[n] e^{-jnT\omega} \\ &= \sum_{n\in\mathbb{Z}} \alpha_k x(nT - \tau_k) e^{-jnT\omega} \\ &= \frac{\alpha_k}{T} \sum_{r\in\mathbb{Z}} X\left(\omega + \frac{2\pi r}{T}\right) e^{-j\left(\omega + \frac{2\pi}{T}r\right)\tau_k}, \end{aligned} \tag{2}$$

where the last equation follows from the Poisson summation formula [7]. Clearly, $Y_k(\omega)$ is a periodic function, with a period of $2\pi/T$.

Since $X(\omega)$ has a finite support, the sum in (2) only contains a finite number of terms. Specifically, consider one period of $Y_k(\omega)$ from $[-B, -B + \frac{2\pi}{T})$, then $Y_k(\omega)$ can be written as

$$Y_k(\omega) = \frac{\alpha_k}{T} \sum_{r=0}^{R-1} X\left(\omega + \frac{2\pi r}{T}\right) e^{-j\left(\omega + \frac{2\pi}{T}r\right)\tau_k}, \tag{3}$$

where $R = \lceil \frac{2BT}{2\pi} \rceil = \lceil \frac{BT}{\pi} \rceil$. In other words, there are only R different shifted versions of $X(\omega)$ in $Y_k(\omega)$. Multiplying both sides of (3) by $e^{j\omega\tau_k}$, we have

$$e^{j\omega\tau_k} Y_k(\omega) = \frac{\alpha_k}{T} \sum_{r=0}^{R-1} X\left(\omega + \frac{2\pi r}{T}\right) e^{-j\frac{2\pi r\tau_k}{T}}. \tag{4}$$

Now, we sample $Y_k(\omega)$ at $\omega_n = -B + \frac{2\pi n}{TN}$, where $n = 0, \ldots, N-1$, and N is the total number of samples. Denote

$$\begin{aligned} \boldsymbol{y}_k &= [Y_k(\omega_0), Y_k(\omega_1), \ldots, Y_k(\omega_{N-1})]^T \in \mathbb{C}^N, \\ \boldsymbol{g}_k &= \left[1, e^{-j\frac{2\pi\tau_k}{TN}}, \ldots, e^{-j\frac{2\pi(N-1)\tau_k}{TN}}\right]^T \in \mathbb{C}^N, \end{aligned} \tag{5}$$

for $k = 1, \ldots, K$, and

$$\boldsymbol{x}_r = \left[X\left(\omega_0 + \frac{2\pi r}{T}\right), \ldots, X\left(\omega_{N-1} + \frac{2\pi r}{T}\right)\right]^T \in \mathbb{C}^N,$$

for $r = 0, \ldots, R-1$, then vectorizing the samples of (4), we have

$$\boldsymbol{g}_k \odot \boldsymbol{y}_k = e^{jB\tau_k} \frac{\alpha_k}{T} \sum_{r=0}^{R-1} e^{-j\frac{2\pi r\tau_k}{T}} \boldsymbol{x}_r, \quad k = 1, \ldots, K. \tag{6}$$

Note that, $\boldsymbol{x}_r$ does not depend on the unknown offsets or gains. The above equation (6) suggests that for all $1 \le k \le K$, $\boldsymbol{g}_k \odot \boldsymbol{y}_k$ lies in the column spans of $\{\boldsymbol{x}_r\}_{r=0}^{R-1}$. Define the matrix $\boldsymbol{Y} = [\boldsymbol{g}_1 \odot \boldsymbol{y}_1, \boldsymbol{g}_2 \odot \boldsymbol{y}_2, \ldots, \boldsymbol{g}_K \odot \boldsymbol{y}_K] \in \mathbb{C}^{N\times K}$, then the subspace-based rank condition [4] states that if $R = \lceil \frac{BT}{\pi} \rceil < K$ and $R = \lceil \frac{BT}{\pi} \rceil \le N$, the matrix $\boldsymbol{Y}$ is rank deficient and has $\operatorname{rank}(\boldsymbol{Y}) \le R$. The first condition requires that the sampling rate $1/T$ should be slightly higher than $1/K$ the Nyquist rate, thus the subsampling ratio per channel is $S \le R < K$. The second condition requires the sampling of the DTFT of $Y_k(\omega)$ to be dense enough.

Based on this rank deficiency of $\boldsymbol{Y}$, Vandewalle et al. [4] proposed an exhaustive search algorithm by testing the rank of $\boldsymbol{Y}$ over all possible combinations of the offsets on a fine grid. The computational complexity of their algorithm grows exponentially with respect to K and the grid size. In [5], Lu and Vetterli took a different approach by writing the first column of $\boldsymbol{Y}$ as a linear combination of the rest of the columns, given as

$$\boldsymbol{y}_1 = \sum_{k=2}^{K} c_k \boldsymbol{y}_k \odot \boldsymbol{g}_k, \tag{7}$$

where we used the fact $\boldsymbol{g}_1$ is an all-one vector since we have assumed $\tau_1 = 0$, and c_k's are unknown coefficients. Note that each $\boldsymbol{g}_k$ in (5) is a complex exponential with the frequency determined by the corresponding offset, so the problem resembles the classical harmonic retrieval problem. Nonetheless, none of the existing methods (e.g. Prony, MUSIC and ESPRIT) can be applied due to the special structure introduced. Lu and Vetterli [5] proposed a very clever algebraic root-finding procedure to estimate the offsets, however, their method requires $N \ge K!$ samples, which is potentially prohibitive when K is large. Moreover, it is well-known that root-finding procedures are sensitive to noise.

III. Proposed Algorithm

In this section, we propose a new algorithm to recover the offsets assuming the subspace-based rank condition holds. To proceed, we first define

$$\boldsymbol{a}(\tau) = \left[1, e^{-j\frac{2\pi\tau}{N}}, \ldots, e^{-j\frac{2\pi\tau(N-1)}{N}}\right]^T \in \mathbb{C}^N,$$

as a complex sinusoid with frequency $\tau \in [0, 1)$. Define a DFT frame with oversampling factor c as

$$\boldsymbol{D} = \left[\boldsymbol{a}(0), \boldsymbol{a}\left(\frac{1}{cN}\right), \ldots, \boldsymbol{a}\left(\frac{cN-1}{cN}\right)\right] \in \mathbb{C}^{N\times cN}.$$

When the oversampling factor is large enough, we approximate the normalized offset $\tau_k/T \approx n_k/(cN) \in [0,1)$ to lie on the DFT frame. Therefore, $\boldsymbol{g}_k$ becomes a 1-sparse vector over the DFT frame, $\boldsymbol{g}_k = \boldsymbol{D}\boldsymbol{c}_k$, where $\boldsymbol{c}_k$ is 1-sparse with the n_kth entry equal to c_k. Consequently, this allows discretization to have minimal effects in our sparse recovery problem, unlike [8]. With this, we can rewrite (7) as

$$\boldsymbol{y}_1 = \sum_{k=2}^{K} \underbrace{\operatorname{diag}(\boldsymbol{y}_k)\,\boldsymbol{D}}_{\boldsymbol{D}_k} \boldsymbol{c}_k = \boldsymbol{G}\boldsymbol{c}, \tag{8}$$

where $\operatorname{diag}(\boldsymbol{y}_k)$ denotes the diagonal matrix with $\boldsymbol{y}_k$ as its diagonal, $\boldsymbol{G} = [\operatorname{diag}(\boldsymbol{y}_2)\,\boldsymbol{D}, \ldots, \operatorname{diag}(\boldsymbol{y}_K)\,\boldsymbol{D}] \in \mathbb{C}^{N \times cN(K-1)}$, and $\boldsymbol{c} = [\boldsymbol{c}_2, \ldots, \boldsymbol{c}_K] \in \mathbb{C}^{cN(K-1)}$.

Therefore, it is possible to recover the offsets by applying sparse recovery algorithms to (8). Note that, the sparse signal $\boldsymbol{c}$ in (8) is structurally sparse, where we know in each block of $\boldsymbol{c}_k$, there is only one nonzero entry. We incorporate this prior information and modify the well-known CoSaMP algorithm [6] to estimate the set of offsets. The algorithm is summarized in Algorithm 1, referred to as the Modified CoSaMP (MCoSaMP) algorithm. Let Υ_k be the index set of the selected columns from $\boldsymbol{D}_k$, then $\boldsymbol{D}_{\Upsilon_k}$ denotes the submatrix constructed by the columns of $\boldsymbol{D}_k$ indexed by Υ_k.

Algorithm 1 Blind Calibration via MCoSaMP

Input: $\boldsymbol{y}_k$, for $k = 1, 2, \ldots, K$, and the DFT frame $\boldsymbol{D}$.
Output: Υ_k, for $k = 2, \ldots, K$.
Initialize: Set $\boldsymbol{D}_k = \operatorname{diag}(\boldsymbol{y}_k)\,\boldsymbol{D}$, $\Upsilon_k = \emptyset$, for $k = 2, \ldots, K$. Set the residual $\boldsymbol{r} = \boldsymbol{y}_1$.
while stopping criterion is not met **do**

1) For $k = 2, \ldots, K$:
   a) $\boldsymbol{p}_k = \boldsymbol{D}_k^H \boldsymbol{r}$;
   b) Set T_k as the indices of the two largest entries of $|\boldsymbol{p}_k|$;
   c) $T_k = \Upsilon_k \cup T_k$.
2) Set $\boldsymbol{D}_T = [\boldsymbol{D}_{T_2}, \boldsymbol{D}_{T_3}, \ldots, \boldsymbol{D}_{T_K}]$.
3) $\boldsymbol{q} = \boldsymbol{D}_T^{\dagger} \boldsymbol{y}_1$.
4) Set Υ_k as the index of the largest entry of $|\boldsymbol{q}_{T_k}|$, for $k = 2, \ldots, K$;
5) $\boldsymbol{D}_u = [\boldsymbol{D}_{\Upsilon_2}, \ldots, \boldsymbol{D}_{\Upsilon_K}]$, $\boldsymbol{q}_u = \left[\boldsymbol{q}_{\Upsilon_2}, \ldots, \boldsymbol{q}_{\Upsilon_{K-1}}\right]^T$.
6) Update $\boldsymbol{r} = \boldsymbol{y}_1 - \boldsymbol{D}_u \boldsymbol{q}_u$.

end

Compared with the original CoSaMP algorithm, we have constrained that in each iteration, we evenly select two more candidates from each block, and then after the least-squares fitting in step 3), we only keep one nonzero entry from each block. The stopping criterion can be set as when the number of maximal iterations is met, or the norm of the residual is small enough. The MCoSaMP algorithm has a computational complexity that is linear with respect to the number of channels K and the grid size, therefore it is very efficient.

When the signal is multi-dimensional, the rank-deficiency condition (7) still holds under appropriate sampling conditions. By discretizing the offsets over the 2-D plane, we can similarly formulate a sparse recovery problem with structured sparsity constraints, for which the MCoSaMP algorithm can be similarly applied. We omit these details due to space constraints, but will provide a numerical experiment in Section IV.

IV. Numerical Experiments

In this section, we carry out a series of numerical experiments to validate the proposed MCoSaMP algorithm and compare its performance with several existing algorithms.

We first compare the performance of the proposed MCoSaMP method with the matrix rank method in [4] and the algebraic root-finding method in [5] when $K = 3$. We set the input signal as $x(t) = \sum_{m=-M}^{M} a_m e^{j2\pi m t}$, where $a_m = a_{-m}^H$, and a_m's are i.i.d. generated from a complex Gaussian distribution for $m = 1, \ldots, M$. For ease of presentation we pick $N = 1/T$ as an integer, so that in each period we obtain N samples from each channel of the multi-channel sampler. We set $M = N - 1$ which represents the largest bandwidth to maintain $R = \lceil \frac{2M+1}{N} \rceil = 2$. Therefore each channel operates at approximately half the Nyquist rate, and we increase the input bandwidth M accordingly in the simulations when we increase the number of samples N. Therefore, the input bandwidth M is increased accordingly when we increase the number of samples N. Furthermore, the samples $y_k[n]$'s are corrupted by additive white Gaussian noise $\mathcal{N}(0, \sigma^2)$, where the SNR is defined as $\log_{10}\left(\sum_{k=1}^{K}\sum_{n=0}^{N-1} y_k[n]^2 / (KN\sigma^2)\right)$ dB. The offsets τ_k's are chosen i.i.d. from a uniform distribution over $[0,1]$, with all gains α_k's set to ones.

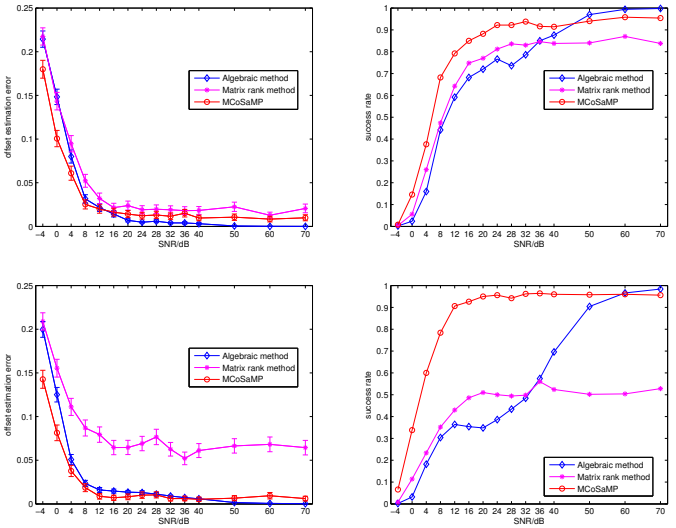

(a) Average offset estimation error (b) Success rate

Fig. 2: The average offset estimation errors and the success rates with respect to SNR for different algorithms when $K = 3$. First row: $N = 128$; second row: $N = 256$.

We examine the three algorithms at each SNR by repeating 500 Monte Carlo simulations. The oversampling factor of the DFT frame is $c = 6$ in the MCoSaMP algorithm. Two

(a) Castle (b) Matrix rank (c) MCoSaMP (d) Cameraman (e) Matrix rank (f) MCoSaMP

Fig. 4: Performance comparisons on image super-resolution. (a) and (d): low-resolution image from one channel; (b) and (e): reconstruction using the matrix rank algorithm [4]; (c) and (f): reconstruction using the proposed MCoSaMP algorithm.

performance metrics are used, the average offset estimation error, defined as $\frac{1}{K-1}\sum_{k=2}^{K}|\tau_k - \hat{\tau}_k|$, where $\hat{\tau}_k$ is the estimate of τ_k, for $k = 2, \ldots, K$; and the success rate, defined as the percentage of trials when the absolute estimation error for each offset is less than 10^{-3}. Fig. 2 shows the performance with respect to SNR of all three algorithms, when $N = 128$ in the first row, and $N = 256$ in the second row. It is clear that the proposed algorithm achieves better performance especially when the SNR is modest. It is also worth noticing that the performance of the matrix rank method and the algebraic method decreases when the bandwidth of the input increases. Next, we examine the effect of input bandwidth on offset

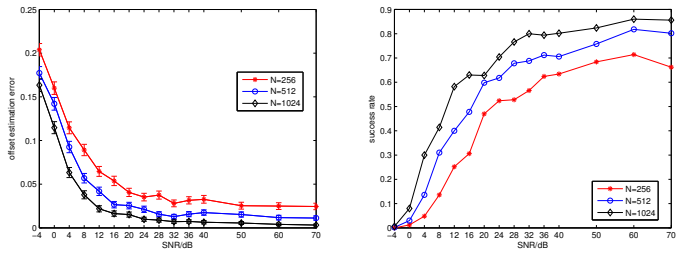

(a) Average offset estimation error (b) Success rate

Fig. 3: The average offset estimation errors and the success rates with respect to SNR for different values of N of the proposed algorithm when $K = 5$.

estimation when $K = 5$. Under the same setup as Fig. 2, we vary the input bandwidth while keeping $R = \lceil \frac{2M+1}{N} \rceil = 4$ by setting $M = 2N-1$. Fig. 3 shows the average offset estimation errors and the success rates of the proposed algorithm when $N = 256, 512, 1024$. It is clear that the performance of the proposed algorithm improves with the increase of input bandwidth.

Finally, we implement the proposed algorithm on image super-resolution and compare it with the heuristic matrix rank method in [4, Section VI, Algorithm 6.2] that is computationally much more efficient. We attempt to reconstruct a 63×63 image from five 32×32 low-resolution images without adding noise. In implementing the proposed MCoSaMP algorithm, we discretize the parameter space $[0, 1]$ of each dimension into 200 uniform grid points. Fig. 4 shows the super-resolution results of a segment of the castle and the cameraman images. Fig. 4 (a) and (d) are one of the five 32×32 low-resolution images, and Fig. 4 (b) and (e) are the super-resolution images using the matrix rank method, and Fig. 4 (c) and (f) are the super-resolution images using the proposed MCoSaMP algorithm. Both algorithms perform comparably well on the castle image, while the proposed algorithm performs much better on the cameraman image. This may happen due to the fact that the heuristic assumptions in [4, Section VI, Algorithm 6.2] may not always hold in practice, while our algorithm does not make additional assumptions.

V. Conclusion

We proposed an efficient algorithm for blind calibration of multi-channel samplers in the presence of unknown gains and offsets, based on a modified CoSaMP algorithm for sparse recovery with a structured sparsity constraint. Numerical examples demonstrate that the proposed algorithm is scalable to more channels, robust to noise, and can handle multi-dimensional signals, making it an appealing choice in practical applications.

Acknowledgements

The authors thank Dr. Vandewalle for providing implementations of the algorithms in [4]. This work is supported by the ONR grant N00014-15-1-2387 and NSF grant CCF-1527456.

References

[1] A. Papoulis, "Generalized sampling expansion," *Circuits and Systems, IEEE Transactions on*, vol. 24, no. 11, pp. 652–654, 1977.

[2] V. Divi and G. Wornell, "Signal recovery in time-interleaved analog-to-digital converters," in *Acoustics, Speech, and Signal Processing, 2004. Proceedings. (ICASSP '04). IEEE International Conference on*, vol. 2, May 2004, pp. ii–593–6 vol.2.

[3] T. Strohmer and J. Xu, "Fast algorithms for blind calibration in time-interleaved analog-to-digital converters," in *Acoustics, Speech and Signal Processing, 2007. ICASSP 2007. IEEE International Conference on*, vol. 3. IEEE, 2007, pp. III–1225.

[4] P. Vandewalle, L. Sbaiz, J. Vandewalle, and M. Vetterli, "Super-resolution from unregistered and totally aliased signals using subspace methods," *Signal Processing, IEEE Transactions on*, vol. 55, no. 7, pp. 3687–3703, 2007.

[5] Y. M. Lu and M. Vetterli, "Multichannel sampling with unknown gains and offsets: A fast reconstruction algorithm," in *Proc. Allerton Conference on Communication, Control and Computing*, Monticello, IL, 2010.

[6] D. Needell and J. A. Tropp, "CoSaMP: Iterative signal recovery from incomplete and inaccurate samples," *Applied and Computational Harmonic Analysis*, vol. 26, no. 3, pp. 301–321, 2009.

[7] J. J. Benedetto and G. Zimmermann, "Sampling multipliers and the poisson summation formula," *Journal of Fourier Analysis and Applications*, vol. 3, no. 5, pp. 505–523, 1997.

[8] Y. Chi, L. Scharf, A. Pezeshki, and A. Calderbank, "Sensitivity to basis mismatch in compressed sensing," *IEEE Transactions on Signal Processing*, vol. 59, no. 5, pp. 2182–2195, May 2011.